

---

## TO STUDY THE FUNCTIONALIZATION OF METAL-ORGANIC FRAMEWORKS ANALYSIS

---

**Setti Rajani**

Research Scholar

Dept of Chemistry, Kalinga University, Raipur, Chhatisgarh

**Dr. Anil Sharma**

Professor

Dept of Chemistry, Kalinga University, Raipur, Chhatisgarh

---

### ABSTRACT

A novel class of hybrid materials called Metal-Organic Frameworks (MOFs) comprised of metals and organic chemicals has a wide range of possible uses. 1 Researchers in chemistry, physics, materials science, and biology have all paid close attention to MOFs since they represent one of the most important advances in solid-state science. Large interior surface areas, ultralow densities, and holes and channels with homogeneous structures characterize these interesting materials, which have drawn an unprecedented amount of study attention over the past ten years. They also have a variety of appealing qualities due to their highly porous<sup>2</sup> and modular construction, and their potential has been investigated in a wide range of applications, including gas storage, catalysis, sensing, separation, removal of hazardous materials, light harvesting, drug delivery, and many others. A central metal atom, typically surrounded by ligands, serves as the building block of a coordination complex. All transition metals, alkaline earth metals, actinides, alkali and metalloids, and lanthanides are studied as part of "coordination chemistry." The ability of metals to attach to various kinds of ligands has led to the development of a huge variety of metal complexes. Because they may bond with diverse metal centers using various coordination sites and enable the effective synthesis of metal complexes, transition metal complexes, which often contain sulfur, oxygen, or nitrogen as ligand atoms, have grown in importance. It is feasible to create a vast array of complexes by combining different amounts of the core metal ions with the surrounding agent ligands.

**KEY WORDS:** *Metal-Organic Frameworks (MOFs), Building Block, Ligand Atoms.*

### INTRODUCTION

The investigation of micro porous metal-organic frameworks (MOFs), which straddle the boundaries of solid-

state chemistry, coordination chemistry, and materials science, has grown into a highly active area of chemical study. The hydrogen-based energy system has been acknowledged by several nations as a partial replacement for the traditional oil-based system. Future production and supply of fossil fuels may be affected by resource depletion. Collateral impact from utilizing fossil fuels includes air pollution. Since hydrogen is a lightweight flammable gas, it may be possible to mitigate some of these negative environmental effects. However, storing hydrogen presents a significant obstacle. The 2015 US DOE hydrogen storage objective has been established at 55 g/g and 40 g/L, with 75 g/g and 70 g/L as the ultimate goals. In addition, the storage system's lifetime is aimed to reach 1500 cycles by 2015; its working temperature should fall between -40 and 85 °C, and its operating pressure should be under 100 bar. Additionally, future automobile generations might be lighter and more fuel-efficient, thus lower numbers below the aim might be feasible. The ability of conventional porous materials like carbons and zeolites to store hydrogen, however, has long been explored. Controlling the environmental impact of anthropogenic emissions will require the development of effective methods for the capture and sequestration of carbon dioxide (CO<sub>2</sub>) produced by current point sources, such as fossil-fuel power plants and blast furnaces. Carbon capture and sequestration (CCS) systems must reduce the energy penalty associated with CO<sub>2</sub> collection and sorbent regeneration and function successfully under actual conditions in order for these technologies to be commercially viable. The quest for materials that meet the requirements of an effective CO<sub>2</sub> sorbent has been moving forward quickly. However, interest in CO<sub>2</sub> capture and conversion as well as hydrogen storage in MOFs is a relatively recent development.

However, over the past few decades, MOFs have drawn the interest of scientists from all over the world, leading to an unparalleled flurry of papers on the subject. More than 10000 MOF structures have been created as a result of the combination of organic and inorganic subunits that results in crystalline porous materials. From the perspective of functional materials, MOFs have attracted a lot of attention for a wide range of practical applications, such as gas storage and separation, catalysis, sensing, conductivity, and light harvesting thanks to their chemical variety and high surface area. Given the variety of MOF structures that have been found, it is important to realize that only a small selection of potential uses for these materials have been explored. According to a fairly recent review, research on MOFs has primarily been concentrated on the identification and characterization of features including luminescence, magnetic properties, and explosives, as well as the discovery of new applications and structurally novel features. Among them, cyclic carbonate synthesis employing MOFs with Polyoxometalates (POMs) and gas storage adsorptive separation are still in their infancy.

The POM clusters in the crystal lattice can be thought of as supramolecular synthons, which is one of the most

intriguing elements of POM chemistry. POMs, which are anionic oxide clusters of early transition metals (Mo, W, V, Nb, Ta, etc.), may have uses in biology, catalysis, and material science. POMs, however, have the capacity to link metal ions with one another via their external oxygen to create network architectures. Most notably, POMs that are employed for acid base catalysis have both Lewis acidic and Lewis basic sites. As a result, POM-incorporated compounds improve the structure's thermal stability in addition to adding functionality. The impregnation approach has been proven successful in the case of MIL-101(Cr) and Cu- BTC, which already have acidic sites as metal clusters in the form of coordinatively unsaturated metal centers (UMC). However, only the large cavities of MIL-101(Cr) can be accessed by Keggin-like structures (13–14 diameter). Given that the medium-sized cavities make up 2/3 of MIL-101(Cr)'s cavity count and that their window openings are smaller than those of Keggin structures, it would appear that encapsulating such active species in these cavities would have many benefits, including improved support utilization and dispersion. Additionally, because polyoxometalates are larger than the windows of these cavities, they would never leak out if POM were contained in the medium cavities. Alcaniz et al. have thoroughly examined the application of MOFs for the encapsulation of various active units. In this article, we describe how polyoxometalates (POM) were enclosed in two Metal Organic Frameworks (MOFs), MIL-101(Cr) [MIL - Material Institute Lavoisier] and Cu-BTC (HKUST-1, – Hong Kong University of Science & Technology). The aforementioned MOFs contained phosphotungstic acid (PTA), a potent heteropoly acid. The ability of these polyoxometalates to adsorb gases as well as their catalytic activity may be improved by the presence of excess metal sites and basic sites (oxides). By adding different amounts of POM to the MOFs, one can also alter the material's ability to store gas. The MOF that was enclosed in POM was made, assessed, and employed as hydrogen storage materials. Gas adsorption characteristics may be influenced by the quantity of polyoxometalates loaded and their orientation in the crystal lattice. Due to the POM's cationic and anionic components' cooperative behavior, there may also be selective H<sub>2</sub> adsorption properties. This could open up new avenues for polyoxometalate-based materials with advantageous catalytic and absorptive characteristics.

Homogeneous catalysis requires high temperatures and pressures, in addition to extra challenges connected to product separation, to produce cyclic carbonate. In contrast, heterogeneous CO<sub>2</sub> fixation catalysts, such as metal oxides, organic, and metal complexes, typically call for extremely high temperatures and/or pressures with numerous purification stages that are significant for a specific chemical process in industry. Traditional catalysts for the cycloaddition reaction include zeolites and mesoporous silica (MCM-41 and SBA-15), which have both acidic and basic sites. The low surface area of these materials results in low yields from these reactions, which

frequently need numerous steps of separation and recycling. Therefore, it is important and difficult to find effective catalysts for the synthesis of cyclic carbonates from CO<sub>2</sub>. In light of this, CO<sub>2</sub> adsorption with in situ conversion, sparked by porous metal-organic frameworks (MOFs), could prove to be a viable tactic for effective and lucrative CO<sub>2</sub> emission reduction. In contrast to conventional catalysts, MOFs have (i) clearly defined and controllable pores, (ii) adaptable architectures, and (iii) the potential to incorporate acid-base sites in addition to having a very large surface area. 28 The potential applications for materials like MIL-101(Cr) as catalysts, gas adsorbents, and storage materials are enormous. The supertetrahedra (ST) building blocks that make up the MIL-101(Cr) hybrid solid are made of trimeric chromium (III) octahedral clusters and stiff terephthalate ligands. The resulting solid consists of two types of quasi-spherical mesoporous cages, the smaller of which has 12 pentagonal faces and the bigger of which has 16 faces. Because MIL-101(Cr) contains coordinatively unsaturated metal sites (CUS), these materials can be used as active sites for research on gas adsorption. Polyoxometalates (POMs) are advantageous options for gas storage from an economic and environmental standpoint due to the existence of surplus metal sites that are crucial for gas adsorption.

It was discovered that [Cu<sub>3</sub>(BTC)<sub>2</sub>-(H<sub>2</sub>O)<sub>x</sub>]<sub>n</sub>, also known as polymeric copper (II) benzene-1,3,5-tricarboxylate, or Cu-BTC, is a highly porous, open-framework metal-coordination polymer. One of the earliest strong metallo-organic polymers with a crucial role in the topology of zeolite frameworks, this substance has a micro porous structure. It consists of dimeric cupric tetracarboxylate units that create a face-centered cubic crystalline framework and an intersecting 3D-channel system. According to earlier research, a substrate's surface carboxylate functional groups may serve as nucleation sites for the formation of MOFs through heterogeneous nucleation and crystal development. Because of the considerable affinity of Li<sup>+</sup> ions for H<sub>2</sub> molecules, both experimental and theoretical studies revealed that the H<sub>2</sub> adsorption capabilities of MOFs can be significantly increased by doping alkali-metal ions, in particular Li<sup>+</sup> ions, to the frameworks. In order to test the H<sub>2</sub> gas adsorption capacity as well as the CO<sub>2</sub> fixation reaction, we therefore planned and made an attempt to dope POM having a high content of metal sites in MOF instead of alkali metal ions. Phosphotungstic acid (PTA) is the POM we select for doping investigations due to its inexpensive cost, ease of availability, and existence of excess metal sites. Both MIL-101(Cr) and Cu-BTC have vacant pores that have been sealed off by PTA to provide the desired characteristics listed above.

## **MATERIALS AND METHOD**

Terephthalic acid, trimesic acid, Cu(NO<sub>3</sub>)<sub>2</sub>·3H<sub>2</sub>O, and Cr(NO<sub>3</sub>)<sub>3</sub>·9H<sub>2</sub>O were acquired from Sigma-Aldrich and

utilized without additional purification. All of the solvents, including acetone, phosphotungstic acid, and N, N'-dimethylformamide (DMF), were purchased from S. D. Fine Chemicals in India. The following sections contain information about spectroscopic and crystallographic studies.

## CHARACTERIZATION

The spectroscopic information below was gathered. In order to acquire data for powder X-ray diffraction (PXRD), a PANalytical Empyrean (PIXcel 3D detector) system with Cu K ( $\lambda = 1.54$  Å) radiation was used. Using an elemental vario MICRO CUBE analyzer, the chemicals were microanalyzed. Using the KBr pellet technique, the samples' infrared spectra (IR) were captured in the 400–4000  $\text{cm}^{-1}$  range using a Perkin-Elmer GX FTIR spectrometer. Using a Mettler Toledo Star SW 8.10 system, thermogravimetric analyses (TGA) (heating rate of 5  $^{\circ}\text{C}/\text{min}$  in nitrogen atmosphere) were carried out. Using the ASAP 2020 surface area and pore size analyzer (Micromeritics Inc., USA) for low pressure gas adsorption measurements on the dehydrated materials, and the automated high pressure gas adsorption equipment BELSORP-HP for high pressure measurements (BEL Inc. Japan). In order to replace lattice guest molecules, samples that had just been manufactured were submerged in low boiling solvents such as acetone and ethanol for five days at room temperature prior to adsorption experiments. Then, to create guest-free samples, the solvent-exchanged frameworks were heated to 120  $^{\circ}\text{C}$  for 6 hours while under vacuum.

## RESULTS AND DISCUSSION

### GENERAL PROCEDURE FOR SYNTHESIS OF MIL-101 (CR) (8)

The MIL-101(Cr) synthetic process described An autoclave was used to sterilize a Teflon® container containing 4 g (0.01 mmol) of Chromium Nitrate,  $\text{Cr}(\text{NO}_3)_3 \cdot 9\text{H}_2\text{O}$ , 1.66 g (0.01 mmol) of Terephthalic Acid-BDC,  $\text{C}_6\text{H}_4$ -1,4-( $\text{COOH}$ )<sub>2</sub>, 0.48 g of Hydrofluoric Acid (HF 40%), and 50 mL of Distilled Water. The autoclave was heated in the following stage for 8 hours at 493 K under static conditions in an oven. The majority of the unreacted terephthalic acids (white crystal) were manually removed using a spatula once the synthesis was finished. Then, ethanol (95% EtOH with 5% H<sub>2</sub>O) was used in a solvothermal/reflux treatment with the remaining green material at 353 K for 24 hours. Finally, the green solid was allowed to dry overnight at 433 K in an environment of air. There is a 1.98g yield. The overall composition of MIL- 101(Cr) can be determined by using the initial molar ratios of the reactants and the elemental analyses (C-24.59, H-5.63). This composition is  $[\text{Cr}_3\text{FO}(\text{BDC})_3(\text{H}_2\text{O})_2]_{25}\text{H}_2\text{O}$ .

**Synthesis of PTA@MIL-101(Cr).**  $[\text{Cr}_3\text{FO}(\text{BDC})_3\text{PW}_{11}\text{O}_{39}\text{H}\cdot(\text{H}_2\text{O})_2]\cdot 25\text{H}_2\text{O}$ , (8').

The following approach, which is already discussed regarding this kind of impregnation process, was described by Ferey et al.<sup>32</sup> 0.4g of activated MIL-101(Cr) and 0.4g of PTA were combined in 10mL of deionized water in the RB, where they were swirled for 24 hours at a speed of 300 rpm. It is then dried in the oven after being repeatedly cleaned with water. There is a 0.65g yield.

**GENERAL PROCEDURE FOR SYNTHESIS OF CU-BTC, (9)**

The synthetic process was adapted somewhat from Q.M. Wang et al.<sup>33</sup>. In a mixture of ethanol and DMF (2.5 + 2.5 mL), 1.13 g of benzene-1, 3, 5-tricarboxylic acid-BTC and 2.42 g of cupric nitrate trihydrate  $\text{Cu}(\text{NO}_3)_2\cdot 3\text{H}_2\text{O}$  were dissolved (5mL). The two solutions were combined for 30 minutes at room temperature before being placed into a condenser-connected 50mL round-bottom (RB) flask. The RB was warmed for 18 hours at 383 K. The RB was then cooled to room temperature, and blue Cu-BTC crystals were separated by filtration before being washed with water and then acetone. At 383K, the product dried for the entire night. There is a 2.15 g yield. The total composition of Cu- BTC can be determined from the initial molar ratios of the reactants and the elemental analyses (C-32.72, H-1.80).

**SYNTHESIS OF PTA@CU-BTC:**  $[\text{Cu}_3(\text{C}_9\text{H}_3\text{O}_6)_2]_4[\{(\text{CH}_3)_4\text{N}\}_4\text{PW}_{11}\text{O}_{39}\text{H}] \cdot 40\text{-H}_2\text{O}$ , (9').

Hill et al.<sup>34</sup> provided the synthetic technique, which was slightly modified.  $\text{Cu}(\text{NO}_3)_2\cdot 3\text{H}_2\text{O}$  (480 mg, 2.50 mmol) and PTA (400 mg, 0.14 mmol) were added to 10 mL of distilled water, and the resultant blue solution was agitated for 10 min. Trimesic acid (420 mg, 2.0 mmol) and  $(\text{CH}_3)_4\text{NOH}$  (362 mg, 2.0 mmol) were added one after the other, followed by 10 minutes of stirring. The resulting pH-3 solution was put into a Teflon-lined autoclave, heated to 200 °C for 20 hours, automatically cooled to 100 °C for an additional 8 hours, and then allowed to cool to room temperature. The resulting deep-blue regular-shaped crystals were taken out of the solution, repeatedly rinsed with distilled water, and then left to soak for three days in acetone. To get rid of water molecules that had become stuck in the product's pores, it was dried in vacuum for an entire night. There is a 232 mg yield.

**FRAMEWORK STRUCTURE AND CHARACTERIZATION**

According to its first report<sup>32</sup>, the structure of MIL-101 is made up of 1,4-BDC anions and Cr(III) trimers, each

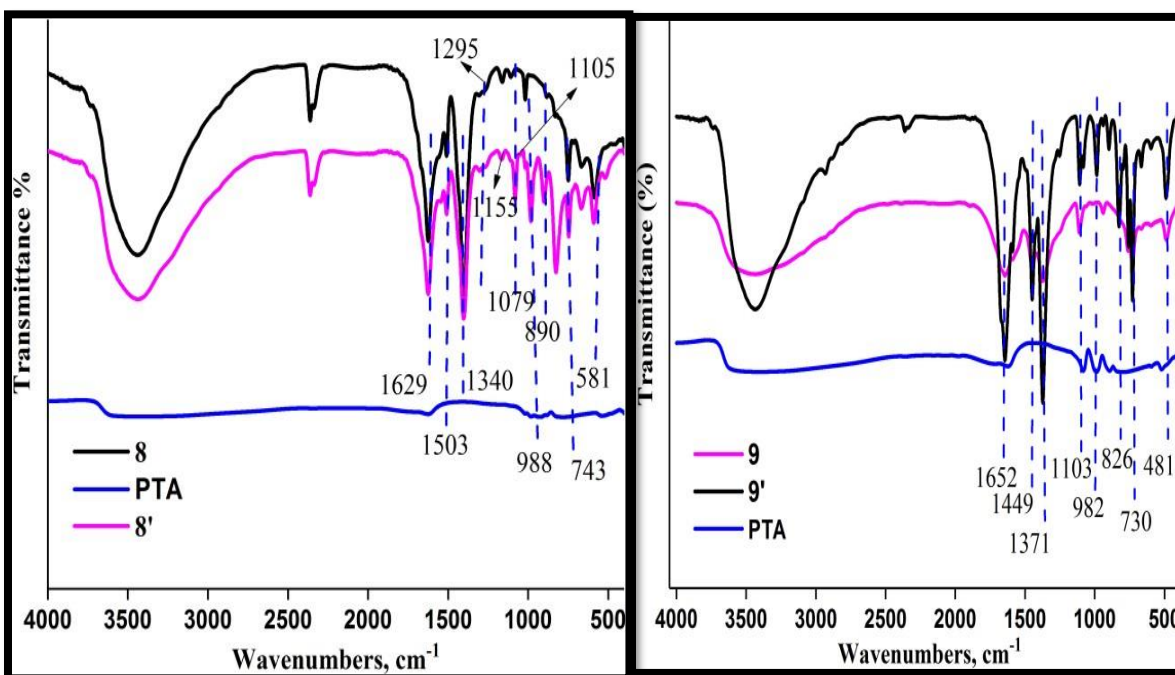


of which has an octahedral environment with four bidentate dicarboxylate oxygen atoms, one 3-O atom, and one fluorine group. These trimeric building blocks are connected by organic linkers to form the large tetrahedron, also known as the super tetrahedron (ST). The resulting framework reveals two distinct mesoporous cages that are present in a 2:1 ratio because the STs are microporous (window aperture: 8.6 Å). The larger cages have both pentagonal and hexagonal windows with 14.5- and 16-Å free apertures, whilst the smaller cages only have pentagonal windows with a 12-Å free opening. As previously mentioned, the vast voids of MIL-101 have been impregnated with polyoxometalates having the Keggin structure. To show the huge volume of such large cavities, lacunary PW11O7-40 anions (one tungsten less than Keggin ion) were added. The impregnation method has been successfully applied to MIL-101, although only its large cavities (13–14 Å diameter) are accessible by Keggin-like structures. It is clear that the encapsulation of such active species into the medium cavities would offer many benefits, including a better dispersion and utilization of the support, given that the medium-sized cavities make up 2/3 of MIL-101's total number of cavities and that their window openings are smaller than those of Keggin structures. Additionally, because the polyoxometalates are larger than the windows of these cavities, leaching of them would never be an issue if confined in the medium cavities.

In a nutshell, the Cu-BTC framework is made up of dimeric cupric tetracarboxylate paddle-wheel units (Cu-Cu = 2.628 Å), where each Cu(II) center exhibits pseudo-octahedral coordination with ligation from four carboxylate groups of various BTC linkers and one H<sub>2</sub>O molecule at the axial position. Three arrays of channels that are perpendicular to one another and intersect at cavities with diameters of 13.2 and 11.1 Å make up the overall structure of this framework. The edges of 12 paddlewheel SBUs line the smaller holes, while the faces of 12 SBUs point inward to the large pores. There are also tiny secondary pores with a 6.9 Å diameter that are surrounded by six SBU edges. Compared to MOF-5, the Cu-BTC exhibits greater thermodynamic stability.<sup>36</sup> The metal-bound water molecules are released when this material is activated, leaving a stable square planar coordination geometry on cupric SBUs. As a result, as seen in scheme 5.2, the color of the framework changes from blue to dark purple. This composite framework reveals a sodalite-type network, in which the Keggin polyoxoanions [PW12O40]<sup>3-</sup> serve as noncoordinating guests, according to single crystal X-ray diffraction (XRD) investigation. Every [PW12O40]<sup>3-</sup> ion is surrounded by six (CH<sub>3</sub>)<sub>4</sub>N<sup>+</sup> cations in the crystal structure.

The MOF and its POM-encapsulated components' FTIR spectra were captured utilizing the KBr pellet method for sample preparation. which depicts a large absorption band between 3000 and 3600 cm<sup>-1</sup> and indicates the presence of firmly bound water in POM-containing materials such as PTA, makes this observation abundantly evident. It also reveals that the naked MIL-101(Cr) material contains this water. The strong band at 1340 cm<sup>-1</sup>

is caused by the symmetric (O-C-O) vibrations of dicarboxylate inside the framework of MIL-101, while the IR vibrational band at 1629  $\text{cm}^{-1}$  reveals the presence of adsorbed water (Cr). The stretching vibration (C=C) at 1503  $\text{cm}^{-1}$  and the deformation vibration (C-H) at 1155, 1079, 890, and 743  $\text{cm}^{-1}$  are both assigned to the benzene ring and appear in the bands between 600 and 1600  $\text{cm}^{-1}$ . The bands close to 580–600  $\text{cm}^{-1}$  are attributed to COO-group in-plane and out-of-plane bending modes. The presence of POMs changes the band at 1155  $\text{cm}^{-1}$ , which is attributed to the Cr-O vibration in MIL-101(Cr). It is typical for PTA-encapsulated MOFs and less intense for bare PTA. The band at 988  $\text{cm}^{-1}$  corresponds to the W=O stretching. 37 The peak at 2360  $\text{cm}^{-1}$  is the result of ambient CO<sub>2</sub> adhering to the surface of the substance. The P-O stretching in unsubstituted H3PW is responsible for the band at 1079  $\text{cm}^{-1}$ , which is clearly present in the loaded samples. This band tends to break into two vibrational absorption bands about 1100  $\text{cm}^{-1}$  when elements like Cr<sup>3+</sup> are included in the structure. The IR spectra of MIL-101(Cr) and Cu-BTC differ slightly because to PTA's encapsulation. The IR spectrum of POM@Cu-BTC (figure 5.1b) perfectly matches the one that Sun et al. previously described. The FTIR spectra of PTA@MIL-101 are depicted in figure (Cr).

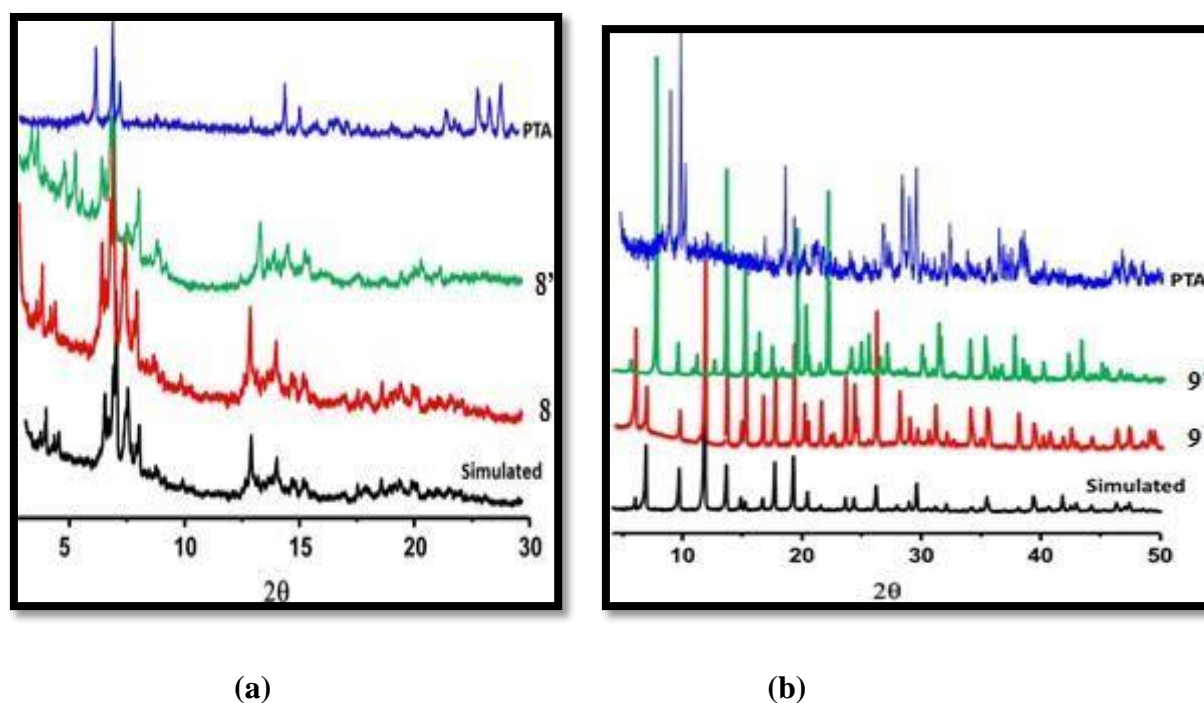


(a) (b)



**Figure 1** FT-IR spectra of (a) **8, 8'**, (b) **9, 9'** with PTA

The simulated patterns of MIL-101(Cr) and Cu-BTC, which clearly distinguish between the bare MIL-101(Cr) and the encapsulated POM such as PTA in MIL-101(Cr), are compared to the XRD patterns of as-synthesized PTA loaded composite materials. Here, for structural information, are the MIL-101(Cr) computed and experimental PXRD patterns. The MIL-101(Cr) structure reported, is supported by the XRD results. Peaks lose some of their intensity as POM loading increases. During the encapsulation of POM, the composite materials formed did not lose their crystalline structure. In stark contrast to the findings published by Sun et al.<sup>38</sup>, the crystal structure appears to remain constant for the MIL-101(Cr) encased samples, and there is also no discernible change in the XRD patterns of Cu-BTC and POM@Cu-BTC through the encapsulation of the POM. Every piece of spectroscopic data suggests that the original POM unit has undergone structural modifications during the encapsulation process, which is consistent with the nature of the encapsulated species. Numerous studies have documented the stability of lacunar POMs by substituting different transition metals for tungsten.

**Figure 2** PXRD patterns of a) **8, 8'** (b) **9, 9'** with PTA

The Cu-BTC XRD pattern and its composite materials' strong agreement and minor peak-to-peak variations showed that the framework structure was preserved even after all of the water molecules were completely

removed.

TGA was used to evaluate the thermal stability and decomposition patterns of the following samples: 8) MIL-101(Cr), 8) PTA @ MIL-101(Cr), 9) Cu-BTC, 9) PTA@Cu-BTC, and PTA in N<sub>2</sub> environment (figure 5.3). It was discovered using thermogravimetric analysis (TGA) that the MIL-101(Cr) is stable up to 350°C. The POM-encapsulated MOF samples' TGA curves are almost identical to those of the bare MOF materials. These materials' TGA plot demonstrates two-step weight decreases. In MIL-101(Cr) and its composites, guest water molecules desorb between 25 and 200 degrees Celsius. A second weight loss is seen between 400 and 600 degrees Celsius due to hydroxyl group dissociation and framework breakdown. The two processes for weight loss are likewise displayed by the Cu-BTC and its composites. As in the case of MIL-101, the first loss is caused by adsorbed water molecules up to 130°C, while the second loss is caused by the disintegration of the framework up to 380°C (Cr). TGA of composite samples also displays a profile that is comparable.

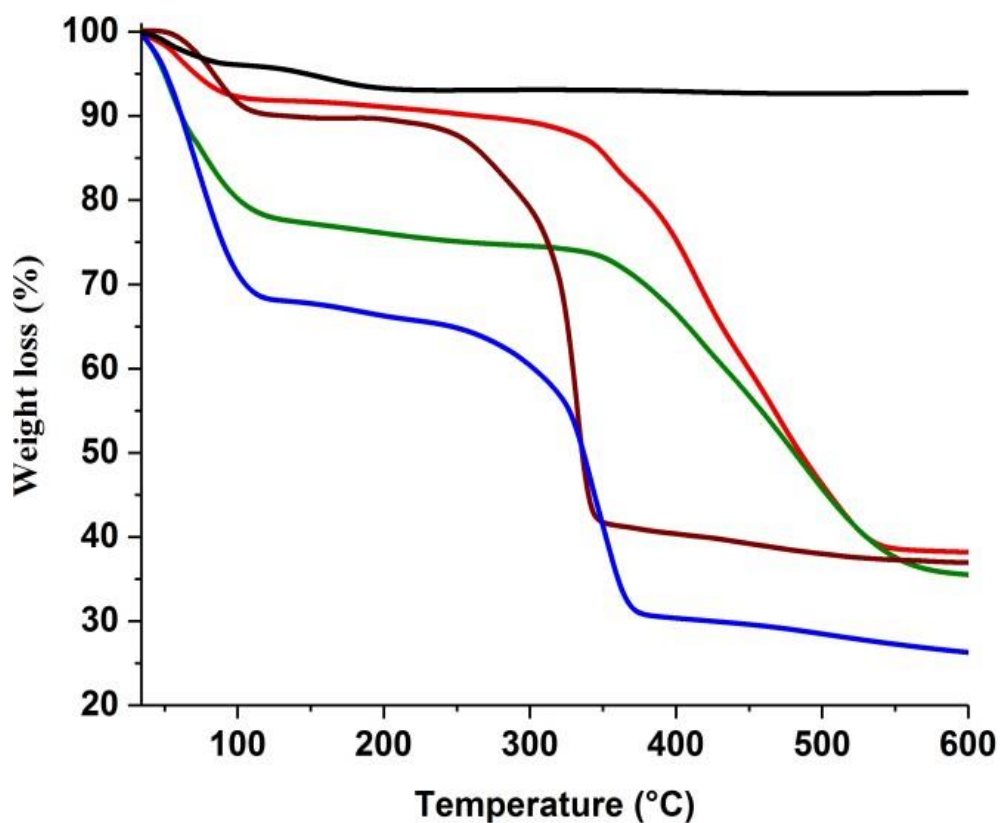


Figure 3 TGA profiles of i) 8 (green), ii) 8' (red), iii) 9 (blue), iv) 9' (brown), v) PTA (black)

The addition of PTA to the synthesis mixture and subsequent hydrothermal treatment allow for the direct encapsulation of PTA in MIL-101(Cr), according to the high resolution transmission electron microscopy HRTEM pictures. The TEM images, however, are consistent with the good dispersion of all the components that were examined. In contrast to MIL-101(Cr), which has larger mesoporous cavities and can hold more PTA units per cavity, Cu-BTC has a structure that only allows one PTA unit to be allocated in each large cavity. The encapsulation of PTA in the MOF is evident in this TEM picture of PTA@Cu-BTC. Red arrows in the TEM pictures point to the PTAs that have been enclosed.

## GAS ADSORPTION

For the N<sub>2</sub> gas sorption analysis at 77 K, 200mg of each composite sample of MIL-101(Cr) and Cu-BTC were evacuated for 5 hours. Cu-BTC and MIL-101(Cr) were heated at 130 °C overnight in a vacuum to eliminate guest solvent molecules from the framework. Prior to the measurement, both samples were once more evacuated for five hours at 120 °C using the surface area analyzer's "degas" function.  $N_{total} = N_{excess} + bulkV_{pore}$ , where bulk is the density of compressed gas at the measured temperature and pressure, and  $V_{pore}$  is derived from the N<sub>2</sub> sorption isotherm at 77 K, was used to compute the total gas intake. Figure 5.6a demonstrates that for both composite materials, a Type I adsorption isotherm was seen without hysteresis. These type I adsorption isotherm cases are a little more complicated, with low pressure steps corresponding to incredibly huge microporous cavities. The fact that the extra at  $P/P_0$  is getting close to 1.0 suggests that tiny macropores have most likely formed between MOF or between composite particles. Due to the filling of two different types of cages with differing amounts of material, the characteristic two-step curve in the adsorption isotherms can be seen. 32. All of the composite MOFs' Brunauer- Emmett-Teller (BET) and Langmuir surface areas, pore sizes, and pore volumes are listed in table -1. The composite sample's N<sub>2</sub> sorption isotherms unmistakably show that the amount of gas adsorption is dependent on the PTA loading ratio. There are 3273 and 2096 m<sup>2</sup>/g of BET surface area, respectively. However, loading PTA results in a decreased pore capacity that matches the mass increase brought on by the addition of PTA. All of the N<sub>2</sub> isotherms that are present on MIL-101(Cr) and its composite materials are type I adsorption isotherms. Additionally, the isotherms of MIL-101(Cr) as-synthesised and MIL-101(Cr) loaded with POM remain unchanged and are fully reversible. Due to the extensive pore volumes' empty character, the surface area of encapsulated Cu-BTC samples (figure 5.6b) is significantly less than that of as-synthesised Cu-BTC (BET surface area: 1340 m<sup>2</sup>/g). These materials' pore volume and size show how microporous they are. The isotherms of PTA@Cu-BTC that were subjected to BET studies (BET surface area: 757 m<sup>2</sup>/g) revealed a consistent reduction in volumetric absorption with regard to increasing

loading ratios of both PTA. The isotherms for Cu-BTC and its composite materials are classified as type I adsorption isotherms. Additionally, in this case, the increased BET surface area was attained by lowering the PTA loading ratio. The reduction in surface area and the pore size distribution as shown in table 5.1 occur in each of the aforementioned instances as a result of the incorporation of POM into the pores of MOFs.

**Figure 4-** N<sub>2</sub> adsorption/desorption isotherms at 77K of (a) **8**, MIL-101(Cr); **8'** PTA@MIL-101(Cr); (b) **9**, Cu-BTC; **9'**, PTA@Cu-BTC. Closed symbols: adsorption; Open symbols: desorption.

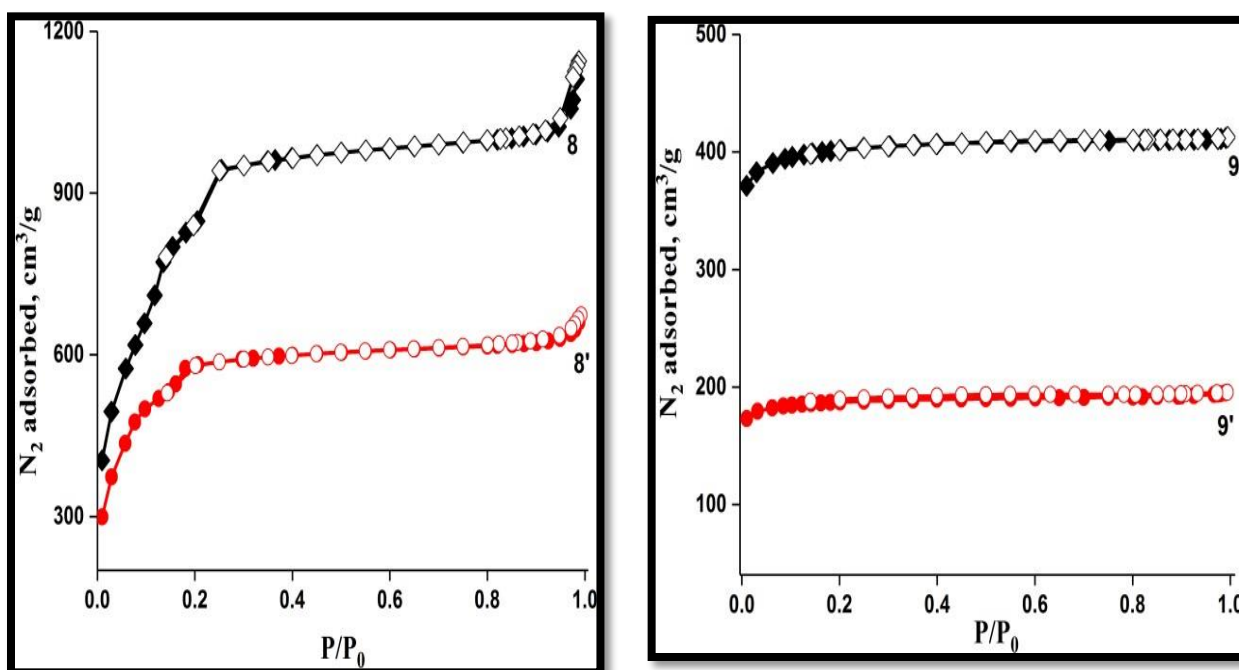


**Table -1** The textural properties of all samples

Serial No	Samples	BET surface area (m <sup>2</sup> /g)	Langmuir surface area m <sup>2</sup> /g	Pore volume (cm <sup>3</sup> /g)	Pore size (nm)	H <sub>2</sub> uptake @77K (Wt. %)	H <sub>2</sub> uptake @303K (Wt. %)
1	MIL-101(Cr) ( <b>8</b> )	3273	4729	1.63	2.97	6.7	0.20
2	PTA@MIL-101(Cr) ( <b>8'</b> )	2096	2896	0.98	2.83	5.4	0.24
3	Cu-BTC ( <b>9</b> )	1340	1773	0.63	2.81	3.3	0.13

4	PTA@Cu-BTC (9')	757	999	0.36	3.66	1.9	0.11
---	--------------------	-----	-----	------	------	-----	------

## CONCLUSION

Encapsulated PTA was effectively produced in MIL-101(Cr) and Cu-BTC. TGA & PXRD patterns demonstrate the heat stability of these composite materials. But when the visitor, such as DMF and water molecules, is removed, the structure remains intact. The N<sub>2</sub> adsorption results show that the loading ratio of the big to medium cavities occupied by the POM is comparable to the ratio in the naked MIL-101(Cr), indicating that both the large and the medium-sized cavities may be employed as hosts for relatively large species. PTA@MIL-101(Cr) (8) and PTA@Cu-BTC (9) reveal hydrogen storage capacities of 5.4 wt% and 1.9 wt%, respectively. However, sample 9 reveals 11.4 wt% and framework 8 displays 23.6 wt% of CO<sub>2</sub> adsorption capacity under ambient conditions, respectively (298K). Overall, the PTA@MIL-101(Cr) (8) solvent-free cycloaddition reactions with co-catalyst TBAB and employing CO<sub>2</sub> and phenyl glycidyl ether demonstrate a synergistic catalysis of 8/TBAB system that resulted in 99% conversion with 97% yield and 99% selectivity. A thorough analysis revealed that 6 hours, a temperature of 100 °C, and pressures of 20 bar of CO<sub>2</sub> were the ideal conditions for achieving the best yield and selectivity for the cyclic carbonate. Additionally, rational variations of both aliphatic and aromatic epoxides show that excellent selectivity and conversion are maintained for practically all substrates under the same reaction conditions. The argument that mesoporous hybrid materials are more effective at CO<sub>2</sub> cycloaddition with smaller as well as bulky epoxides is further supported by this.

## REFERENCES

1. IUPAC, Compendium of Chemical Terminology, 2nd ed. (the "GoldBook") (1997).
2. IUPAC, Compendium of Chemical Terminology, 2nd ed. (the "GoldBook") (1997).
3. Thompson KH Encyclopedia of Inorganic Chemistry. In: King RB (ed.), John Wiley & Sons Ltd., Chichester, UK. 2011.
4. Natarajan Raman, Sivasangu Sobha, Liviu Mitu. Springer, MonatshChem., **143** (2012) 1019
5. Jurisson S, Berning D W, Ma D S. Chem, Rev., **93** (1993)1137
6. Rey A M, Curr. Med, Chem., **17** (2010) 3673
7. Zhen Z P, Tang W, Guo C L, Chen H M, Lin X, Liu G, Fei B W, Chen XY, Xu B Q, Xie J, J, ACS Nano., **7** (2013) 6988

8. Becker J J, Gagne M R, *Acc,Chem,Res.*, **37** (2004) 798
9. Ramaswamy N, Tylus U, Jia M R, *S. J.Am,Chem, Soc.*, **135** (2013) 15443
10. [35] Wenger O S, *Chem,Rev.*, **113** (2013) 3686
11. Wei H, Chen C G, Han H Y, Wang E K. *Anal, Chem.*, **80** (2008) 7051
12. Wei H, Li B L, Du Y, Dong S J, Wang E. *Chem, Mater.*, **19** (2007) 2987
13. Wei H, Wang E K. *Nanotechnology.*, **18** (2007) 295
14. Wei H, Li J, Wangand Y L, Wang E K, *Nanotechnology.*, **18** (2007) 175
15. Wei H, Wang E K, Hou C J, Lu Y. *Analyst.*, **135** (2010) 1406
16. Wei H, Y G, Yang L M, Tan L H, Hou C J, *Nat, Nanotechnol.*, **6** (2011) 93
17. [42] Li C C, Zeng H C. *J, Am,Chem, Soc.*, **134** (2012) 19084
18. Gianneschi N C, Masar M S, Mirkin C A. *Acc,Chem, ReS.*, **38** (2005) 825
19. Wang C, Tan E N, Zhang Y Y, Yu Y H, Li Z Y, *Chem,Sci.*, **5** (2014)1225
20. Song Y H, Wei G, Wang L, Sun Y L, *J,Phys,Chem, B.*, **111** (2007) 461
21. Song Y H, Li Z, Liu Z G, Wei G, *J,Phys,Chem, B.*, **110** (2006) 10792
22. Shuyu Zhang, Yubin Ding and Hui Wei, *Molecules.*, **19** (2014) 11933
23. Oxana V, Kharissova, Méndez-Martínez. *Molecules.*, **19** (2014) 10755